

Searching for strange hidden-charm pentaquark state $P_{cs}(4459)$ in $\gamma p \rightarrow K^+ P_{cs}(4459)$ reaction

Cai Cheng¹, Feng Yang², and Yin Huang^{2,3*}

¹ School of Physics and Electronic Engineering, Sichuan Normal University, Chengdu 610101, China

² School of Physical Science and Technology, Southwest Jiaotong University, Chengdu 610031, China and

³ Asia Pacific Center for Theoretical Physics, Pohang University of Science and Technology, Pohang 37673, Gyeongsangbuk-do, South Korea.

(Dated: November 16, 2021)

We investigate the possibility of studying the strange hidden-charm pentaquark state $P_{cs}(4459)$ by photon-induced reactions on a proton target in an effective Lagrangian approach. The production process is described by the t -channel K^- exchange, the u -channel Λ exchange, the contact term, and the s -channel nucleon pole. Our theoretical approach is based on the assumption that $P_{cs}(4459)$ with $J^P = 1/2^-$ or $J^P = 3/2^-$ can be interpreted as a molecule composed of $\bar{D}^*\Xi_c$. Using the coupling constants of the $P_{cs}^{J^P}$ to $\gamma\Lambda$ and K^-p channels obtained from molecule picture of the $P_{cs}^{J^P}(4459)$, the total cross-sections of the process $\gamma p \rightarrow P_{cs}^{J^P} K^+$ is evaluated. Our calculation indicates that the cross-section for $\gamma p \rightarrow P_{cs}^{1/2^-} K^+$ and $\gamma p \rightarrow P_{cs}^{3/2^-} K^+$ are of the order of 10.0 pb and 5.0 pb, respectively. In addition, we compute the cross-section by assuming $P_{cs}(4459)$ as a compact pentaquark and find it is quite different from the results of $\bar{D}^*\Xi_c$ molecule. Those results can be measured in future experiments, such as the Electron-Ion Collider in China and the United States. And can be used to test the nature of the P_{cs} .

PACS numbers:

I. INTRODUCTION

In decades, more and more hadronic exotic states were observed following the accumulation of the precise data in high energy experiments [1]. These hadrons have an internal structure more complex than the simple $\bar{q}q$ configuration for mesons or the qqq configuration for baryons in the traditional picture of the constituent quark models. Studying the exotic hadron states is not only conducive to the development of the hadron spectrum but also provides an important opportunity for us to better understand the strong interaction.

Very recently, the LHCb experiment reported a new hadronic exotic state, namely $P_{cs}(4459)$, in the $J/\psi\Lambda$ invariant mass distributions of the $\Xi_b^- \rightarrow J/\psi\Lambda K^-$ decay [2]. The mass and width of the $P_{cs}(4459)$ are measured to be

$$\begin{aligned} M &= 4458.8 \pm 2.9_{-1.1}^{+4.7} \text{ MeV}, \\ \Gamma &= 17.3 \pm 6.5_{-5.7}^{+8.0} \text{ MeV}, \end{aligned} \quad (1)$$

respectively. From the $J/\psi\Lambda$ decay mode, the new structures $P_{cs}(4459)$ contain at least five valence quarks with isospin is zero. Because the quark components of J/ψ meson and Λ baryon are $\bar{c}c$ and uds , respectively, the $P_{cs}(4459)$ is another new candidate of hidden-charm pentaquark states following the previous discovery of three hidden-charm pentaquark states [3, 4]. However, its spin-parity quantum number was not confirmed since the statistics is not large enough.

The discovery of the first strange hidden-charm pentaquark immediately intrigues an active discussion on its structure. Among the theoretical pictures in the field, the molecular picture is a competitive one to explain existing candidates of exotic states. The idea comes from the molecular state interpretation of the deuteron, as the deuteron mass is a little below

the corresponding threshold and exhibit a sizable spatial extension. It immediately leads to a conclusion that a molecular state is close to the threshold of constituent hadrons. This feature can be used for defining a hadronic molecule. Along this line, one can find that the mass difference between the $P_{cs}(4459)$ and $\bar{D}^*\Xi_c$ threshold is about 19 MeV, which indicates the $P_{cs}(4459)$ could be a candidate for the $\bar{D}^*\Xi_c$ molecular state.

Indeed, the QCD sum rules support its interpretation as the $\bar{D}^*\Xi_c$ hadronic molecular state of either $J^P = 1/2^-$ or $3/2^-$ [5]. Using the coupled channel unitary approach combined with heavy quark spin and local hidden gauge symmetries, Ref. [6] find a pole of $4459.07 + i6.89$ MeV below the $\bar{D}^*\Xi_c$ threshold consistent with the mass and width of the $P_{cs}(4459)$ state. In Ref. [7], the $P_{cs}(4459)$ was regarded as a $\bar{D}^*\Xi_c$ molecular pentaquark state with $J^P = 3/2^-$, or possibly $J^P = 1/2^-$ with more uncertainties about its mass. The partial decay width of the molecular $P_{cs}(4459)$ into $J/\psi\Lambda$ is predicted to be larger for the $J^P = 3/2^-$ configuration than the $J^P = 1/2^-$ case, in agreement with the conclusions in Refs. [6, 8]. With the quasipotential Bethe-Salpeter equation approach, Ref. [9] assigned the $P_{cs}(4459)$ state to the $\bar{D}^*\Xi_c$ molecular state with $J^P = 3/2^-$. By using a one-boson-exchange model, Ref. [10] concluded that the $P_{cs}(4459)$ state is not a pure $\bar{D}^*\Xi_c$ molecular state. This is the same with our result [8] that the $P_{cs}(4459)$ can be explained as S -wave coupled molecular state with $J^P = 3/2^-$. We also proposed that a pure $\bar{D}^*\Xi_c$ molecular state with mass about 4459 and $J^P = 1/2^-$ could exist, and it mainly decays to $D\Xi_c'$ final state.

Its properties, however, such as the spectroscopy and the decay width, can be well explained in the context of the multi-quark state [11–13] with the conclusion that the $P_{cs}(4459)$ can be assigned as hidden charm compact pentaquark state with $J^P = 1/2^-$ or $J^P = 3/2^-$. We also noted that before the LHCb observation [2], the $P_{cs}(4459)$ state mass has been calculated in Ref. [14] with an extension of the Gürsey and Radicati mass formula [15]. In this paper the authors suggested also to

*Electronic address: huangy2019@swjtu.edu.cn; yin.huang@apctp.org

search for P_{cs} states in the $\Xi_b^- \rightarrow J/\Psi \Lambda K^-$ channel and calculated the $P_{cs}(4459) \rightarrow J/\Psi \Lambda$ strong partial decay widths [14] with assumption that $P_{cs}(4459)$ is a compact pentaquark state.

An urgent question of high relevance is to understand the nature of this state: how to distinguish the various interpretations. One way to distinguish the various interpretations of the $P_{cs}(4459)$ is to study its production processes. The present knowledge about the $P_{cs}(4459)$ was obtained from the pp collision [2]. High energy photon beams are available at Electron-Ion Collider in China (EicC) [16] or in the United States (US-EIC) [17], which provide another alternative to studying $P_{cs}(4459)$. Thus, it will be helpful to understand the nature of the $P_{cs}(4459)$ if we can observe this state in $\gamma p \rightarrow P_{cs}(4459)^0 K^+$ production processes. The production of the $P_{cs}(4459)$ via a kaon-induced reaction on a nucleon target was discussed in Ref. [18].

This paper is organized as follows. In Sec. II, we will present the theoretical formalism. In Sec. III, the numerical result will be given, followed by discussions and conclusions in the last section. The Appendix contains technical details to compute the partial decay widths of $P_{cs} \rightarrow \gamma \Lambda$ and $P_{cs} \rightarrow K^- P$ reactions.

II. THEORETICAL FORMALISM

A. P_{cs} production as $\bar{D}^* \Xi_c$ molecule

In this work, we study the process $\gamma p \rightarrow P_{cs}(4459)^0 K^+$ within the effective Lagrangian approach, which has been widely employed to investigate photoproduction processes. The relevant Feynman diagrams for the process $\gamma p \rightarrow P_{cs}(4459)^0 K^+$ are depicted in Fig. 1. Here we take into account the nucleon-pole contribution in the s -channel, the Λ -pole contribution in the u -channel, and K exchanges in the t -channel. To ensure the gauge invariance of the total amplitudes, the contact diagram must be included.

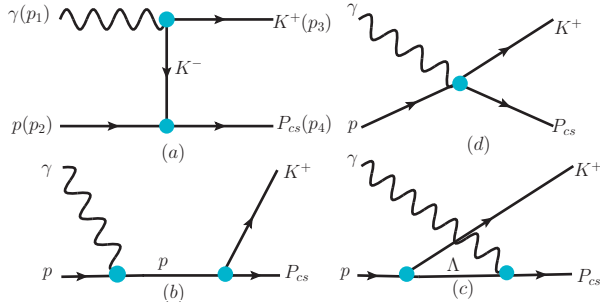


FIG. 1: Feynman diagrams for the process $\gamma p \rightarrow K^+ P_{cs}(4459)$. The contributions from the t -channel K^- exchange (a), s -channel nucleon pole (b), u -channel Λ hadron (c), and contact term (d) are considered. In the first diagram, we also show the definition of the kinematics (p_1, p_2, p_3, p_4) that we use in the present calculation.

To compute the amplitudes of the diagrams shown in Fig. 1, we need the effective Lagrangian densities for the relevant

interaction vertices. The spin parity of the $P_{cs}(4459)$ state was still not determined in experiments. The theoretical studies suggested that possible assignments of spin parity of the $P_{cs}(4459)$ are $J^P = 1/2^-$ and $3/2^-$ [5–13]. In this work, we will consider these two possibilities. Taking into account these different quantum numbers, we can express the interactions by the effective Lagrangians [18–20]

$$\mathcal{L}_{KNP_{cs}}^{1/2^-} = -g_{KNP_{cs}} \bar{P}_{cs} N K + H.c., \quad (2)$$

$$\mathcal{L}_{KNP_{cs}}^{3/2^-} = -\frac{g_{KNP_{cs}}}{m_N m_{P_{cs}}} \epsilon^{\mu\nu\alpha\beta} \partial_\mu \bar{P}_{cs, \nu} \gamma_\alpha N \partial_\beta K + H.c., \quad (3)$$

$$\mathcal{L}_{\gamma\Lambda P_{cs}}^{1/2^-} = \frac{eh}{2m_\Lambda} \bar{\Lambda} \sigma_{\mu\nu} \partial^\nu \mathcal{A}^\mu P_{cs} + H.c., \quad (4)$$

$$\mathcal{L}_{\gamma\Lambda P_{cs}}^{3/2^-} = -e \left(\frac{ih_1}{2m_\Lambda} \bar{\Lambda} \gamma^\nu + \frac{h_2}{(2m_\Lambda)^2} \partial^\nu \bar{\Lambda} \right) \mathcal{F}_{\mu\nu} P_{cs}^\mu + H.c., \quad (5)$$

$$\mathcal{L}_{\gamma KK} = -ie (K^- \partial^\mu K^+ - K^+ \partial^\mu K^-) \mathcal{A}_\mu, \quad (6)$$

$$\mathcal{L}_{\gamma PP} = -e \bar{p} (\mathcal{A} - \frac{\kappa_p}{2m_N} \sigma_{\mu\nu} \partial^\nu \mathcal{A}^\mu) p + H.c., \quad (7)$$

$$\mathcal{L}_{KPA} = \frac{g_{KNA}}{m_N + m_\Lambda} \bar{p} \gamma^\mu \gamma_5 \Lambda \partial_\mu K^+ + H.c., \quad (8)$$

with $\mathcal{F}^{\mu\nu} = \partial_\mu \mathcal{A}_\nu - \partial_\nu \mathcal{A}_\mu$, $\sigma^{\mu\nu} = \frac{i}{2} (\gamma^\mu \gamma^\nu - \gamma^\nu \gamma^\mu)$, and the electromagnetic fine structure constant $\alpha = e^2/4\pi = 1/137$. The anomalous magnetic moment reads $\kappa_p = 1.79$, and $\epsilon^{\mu\nu\alpha\beta}$ is the Levi-Civita tensor with $\epsilon^{0123} = 1$. P_{cs} , Λ , N , \mathcal{A} , and K are the P_{cs} state, Λ baryon, nucleon, photon, and K meson fields, respectively. $m_{P_{cs}}$, m_Λ , and m_N represent the masses of $P_{cs}(4459)$, Λ , and the nucleon, respectively.

Here, we discuss relevant coupling constants that we need. First, the coupling constant g_{KNA} can be determined by flavor $SU(3)$ symmetry relations, which give $g_{KNA} = 13.4$ [21, 22]. According to the quark components of $P_{cs}(4459)$ and Λ , the decay of the P_{cs} state into $\gamma \Lambda$ should perform via the $c\bar{c}$ annihilation. For the $P_{cs}(4459)$ with $J^P = 3/2^-$, there are two different coupling structures for the vertex $P_{cs} \Lambda \gamma$. Their values can be computed by the radiative decay width of $P_{cs}^{3/2^-} \rightarrow \gamma \Lambda$, which is obtained from Eq. (5)

$$\Gamma(P_{cs}^{3/2^-} \rightarrow \gamma \Lambda) = \frac{e^2 |\vec{p}_\gamma|^3}{12\pi} \left\{ \frac{h_1^2}{4m_\Lambda^2} \left(3 + \frac{m_\Lambda^2}{m_{P_{cs}}^2} \right) + \left(1 + \frac{m_\Lambda}{m_{P_{cs}}} \right) \right. \\ \left. \times \left[\frac{h_1 h_2 m_{P_{cs}}}{8m_\Lambda^3} \left(3 + \frac{m_\Lambda}{m_{P_{cs}}} \right) + \frac{h_2^2 m_{P_{cs}}^2}{16m_\Lambda^4} \left(1 + \frac{m_\Lambda}{m_{P_{cs}}} \right) \right] \right\}, \quad (9)$$

where $|\vec{p}_\gamma|$ is the photon three momenta in the center of mass frame.

As argued in Refs. [19, 20], for hidden charm pentaquark state decays into $J/\psi p$ the momentum of the final states are fairly small compared to the nucleon mass. Thus, the higher partial wave terms proportional to $(p/m_N)^2$ and $(p/m_N)^3$ can be neglected. It means that the value of the coupling constant h_2 related to the higher partial wave term is zero. In this work we will only consider the leading order s -wave $P_{cs}^{3/2^-} \Lambda \gamma$ coupling and leave the higher partial waves to further studies by following the same pattern in Refs. [19, 20]. Thus, we can

relate h_1 to the radiative decay width of $P_{cs}^{3/2^-} \rightarrow \gamma\Lambda$

$$\Gamma(P_{cs}^{3/2^-} \rightarrow \gamma\Lambda) = \frac{e^2 |\vec{p}_\gamma^3| h_1^2}{12\pi 4m_\Lambda^2} \left(3 + \frac{m_\Lambda^2}{m_{P_{cs}}^2}\right). \quad (10)$$

However, only one coupling structure exist for the P_{cs} (4459) with $J^P = 1/2^-$. With the help of Eq. (4), the coupling constant h can be determined by the radiative decay width of $P_{cs}^{1/2^-} \rightarrow \gamma\Lambda$

$$\Gamma(P_{cs}^{1/2^-} \rightarrow \gamma\Lambda) = \frac{e^2 h^2}{4\pi m_\Lambda^2} |\vec{p}_\gamma^3|. \quad (11)$$

The coupling constants of $g_{KNP_{cs}}$ are needed as well in our calculation. The decay processes of $P_{cs} \rightarrow K^- p$ are calculated and the relevant coupling constants $g_{KNP_{cs}}$ can be obtained from their partial decay widths with different J^P assignments of the P_{cs} states. The decay rates read

$$\Gamma(P_{cs}^{1/2^-} \rightarrow K^- p) = \frac{g_{KNP_{cs}}^2 (m_{P_{cs}} + m_N)^2 - m_{K^-}^2}{8\pi m_{P_{cs}}^2} |\vec{p}|_{K^-}, \quad (12)$$

$$\Gamma(P_{cs}^{3/2^-} \rightarrow K^- p) = \frac{g_{KNP_{cs}}^2 (m_{P_{cs}} - m_N)^2 - m_{K^-}^2}{24\pi m_N^2 m_{P_{cs}}^2} |\vec{p}|_{K^-}^3, \quad (13)$$

where M_{K^-} is the masses of the K^- meson and $|\vec{p}|_{K^-}$ is the three-momenta of the decay products in the center of mass frame.

In evaluating the production amplitudes of the $\gamma p \rightarrow K^+ P_{cs}$ reaction, we need to include the form factors because hadrons are not pointlike particles. For the t -channel K^- meson exchange diagram, we take the form factor as [22]

$$\mathcal{F}_M(q_{ex}, m_{ex}) = \left[\frac{\Lambda_M^2 - m_{ex}^2}{\Lambda_M^2 - q_{ex}^2} \right]^m. \quad (14)$$

For s - and u -channel diagrams, we adopt the form factor [21, 22]

$$\mathcal{F}_B(q_{ex}, m_{ex}) = \left[\frac{n\Lambda_B^4}{n\Lambda_B^4 + (q_{ex}^2 - m_{ex}^2)^2} \right]^n, \quad (15)$$

which approaches a Gaussian form as $n \rightarrow \infty$. q_{ex} and m_{ex} are the four-momentum and the mass of the exchanged particle, respectively. Λ_M , Λ_B , m and n will be taken as parameters and discussed later.

With the vertices Lagrangian densities described in Eqs. (2)-(8), we can further work out the scattering amplitudes

of the $\gamma p \rightarrow K^+ P_{cs}$ reaction

$$\begin{aligned} \mathcal{M}_a^{1/2^-} &= -ie g_{KNP_{cs}}^{1/2^-} \bar{u}(p_4, s_{cs}) u(p_2, s_2) \frac{1}{q_t^2 - m_{K^-}^2} \\ &\times (p_3^\mu - q_t^\mu) \epsilon_\mu(p_1, s_1) \mathcal{F}_{K^-}(q_t), \end{aligned} \quad (16)$$

$$\begin{aligned} \mathcal{M}_b^{1/2^-} &= ie g_{KNP_{cs}}^{1/2^-} \bar{u}(p_4, s_{cs}) \frac{\not{q}_s + m_p}{q_s^2 - m_p^2} \left[\gamma^\mu - \frac{\kappa_p}{4m_p} (\gamma^\mu \not{p}_1 - \not{p}_1 \gamma^\mu) \right] \\ &\times u(p_2, s_2) \epsilon_\mu(p_1, s_1) \mathcal{F}_N(q_s), \end{aligned} \quad (17)$$

$$\begin{aligned} \mathcal{M}_c^{1/2^-} &= -\frac{eh g_{KN\Lambda}^{1/2^-}}{4m_\Lambda(m_p + m_\Lambda)} \bar{u}(p_4, s_{cs}) (\gamma^\mu \not{p}_1 - \not{p}_1 \gamma^\mu) \\ &\times \frac{\not{q}_u + m_\Lambda}{q_u^2 - m_\Lambda^2} \not{p}_3 \gamma_5 u(p_2, s_2) \epsilon_\mu(p_1, s_1) \mathcal{F}_\Lambda(q_u), \end{aligned} \quad (18)$$

$$\mathcal{M}_d^{1/2^-} = ie g_{KNP_{cs}}^{1/2^-} \bar{u}(p_4, s_{cs}) \mathcal{C}_{1/2^-}^\mu \epsilon_\mu(p_1, s_1) u(p_2, s_2) \quad (19)$$

and

$$\begin{aligned} \mathcal{M}_a^{3/2^-} &= -i \frac{e g_{KNP_{cs}}^{3/2^-}}{m_p m_{P_{cs}}} e^{\mu\nu\alpha\beta} p_{4\mu} q_{t\beta} (p_3^\rho - q_t^\rho) \epsilon_\rho(p_1, s_1) \mathcal{F}_{K^-}(q_t) \\ &\times \frac{1}{q_t^2 - m_{K^-}^2} \bar{u}_\nu(p_4, s_{cs}) \gamma_\alpha u(p_2, s_2), \end{aligned} \quad (20)$$

$$\begin{aligned} \mathcal{M}_b^{3/2^-} &= -i \frac{e g_{KNP_{cs}}^{3/2^-}}{m_p m_{P_{cs}}} e^{\mu\nu\alpha\beta} p_{4\mu} p_{3\beta} \epsilon_\rho(p_1, s_1) \mathcal{F}_N(q_s) \bar{u}_\nu(p_4, s_{cs}) \\ &\times \gamma_\alpha \frac{\not{q}_s + m_p}{q_s^2 - m_p^2} \left[\gamma^\rho - \frac{\kappa_p}{4m_p} (\gamma^\rho \not{p}_1 - \not{p}_1 \gamma^\rho) \right] u(p_2, s_2), \end{aligned} \quad (21)$$

$$\begin{aligned} \mathcal{M}_c^{3/2^-} &= \frac{eh_1 g_{KNP_{cs}}^{3/2^-}}{2m_\Lambda(m_\Lambda + m_p)} \epsilon_\rho(p_1, s_1) \mathcal{F}_\Lambda(q_u) \bar{u}_\mu(p_4, s_{cs}) \\ &\times (p_1^\mu \gamma^\rho - \not{p}_1 g^{\mu\rho}) \frac{\not{q}_u + m_\Lambda}{q_u^2 - m_\Lambda^2} \not{p}_3 \gamma_5 u(p_2, s_2), \end{aligned} \quad (22)$$

$$\begin{aligned} \mathcal{M}_d^{3/2^-} &= i \frac{e g_{KNP_{cs}}^{3/2^-}}{m_p m_{P_{cs}}} e^{\mu\nu\alpha\beta} p_{4\mu} \bar{u}_\nu(p_4, s_{cs}) \mathcal{C}_{3/2^-}^{\beta\rho} \gamma_\alpha u(p_2, s_2) \\ &\times \epsilon_\rho(p_1, s_1), \end{aligned} \quad (23)$$

where $q_s = p_1 + p_2 = p_3 + p_4$, $q_t = p_1 - p_3 = p_4 - p_2$ and $q_u = p_2 - p_3 = p_4 - p_1$. The $\mathcal{C}_{1/2^-}^\mu$ and $\mathcal{C}_{3/2^-}^{\beta\rho}$ are introduced to ensure that the full photoproduction amplitude satisfies the generalized Ward-Takahashi identity and thus is fully gauge invariant. Here, we choose

$$\mathcal{C}_{1/2^-}^\mu = \frac{2\mathcal{F}_{K^-}(q_t)}{q_t^2 - m_{K^-}^2} p_3^\mu - \frac{2\mathcal{F}_N(q_s)}{q_s^2 - m_p^2} p_2^\mu, \quad (24)$$

$$\mathcal{C}_{3/2^-}^{\beta\rho} = \frac{2\mathcal{F}_{K^-}(q_t)}{q_t^2 - m_{K^-}^2} p_3^\rho q_t^\beta + \frac{2\mathcal{F}_N(q_s)}{q_s^2 - m_p^2} p_2^\rho p_3^\beta. \quad (25)$$

The differential cross section in the center of mass (c.m.) frame for the process $\gamma p \rightarrow P_{cs} K^+$ is calculated using

$$\frac{d\sigma}{d\cos\theta} = \frac{m_N m_{P_{cs}} |\vec{p}_3^{\text{c.m.}}|}{32\pi q_s^2 |\vec{p}_1^{\text{c.m.}}|} \sum_{s_1, s_2, s_3, s_4} |\mathcal{M}^{J^P=1/2^-, 3/2^-}|^2 \quad (26)$$

where $\mathcal{M}^{J^P} = \mathcal{M}_a^{J^P} + \mathcal{M}_b^{J^P} + \mathcal{M}_c^{J^P} + \mathcal{M}_d^{J^P}$ is the total scattering amplitude of the $\gamma p \rightarrow P_{cs} K^+$ reaction. θ is the scattering

angle of the outgoing K^+ meson relative to the beam direction, while $\vec{p}_1^{x,m}$ and $\vec{p}_3^{x,m}$ are the photon and K^+ meson three momenta in the c.m. frame, respectively, which are

$$|\vec{p}_1^{x,m}| = \frac{\lambda^{1/2}(q_s^2, 0, m_N^2)}{2\sqrt{q_s^2}}; \quad |\vec{p}_3^{x,m}| = \frac{\lambda^{1/2}(q_s^2, m_{K^+}^2, m_{P_{cs}}^2)}{2\sqrt{q_s^2}} \quad (27)$$

where the λ is the Källén function with $\lambda(x, y, z) = (x - y - z)^2 - 4yz$.

B. P_{cs} production as compact pentaquark

It is helpful if we could estimate the cross-section to make a comparison by assuming $P_{cs}(4459)$ as a compact pentaquark. Thus, we can judge the different explanations for the structure of $P_{cs}(4459)$ if there exist experimental signals. Fortunately, a compact pentaquark P_{cs}^0 with a mass of about 4520 ± 47 MeV and isospin $I = 0$ is predicted [14]. And the decay width of this state into $J/\psi\Lambda$ is 7.94 MeV [14]. Considering it as one particle, which is $P_{cs}(4459)$ found in the LHCb experiment[2], the cross-section of the process $\gamma p \rightarrow P_{cs}K^+$ can be computed with the vector meson dominance mechanism and relevant Feynman diagrams plotted in Fig. 3. The

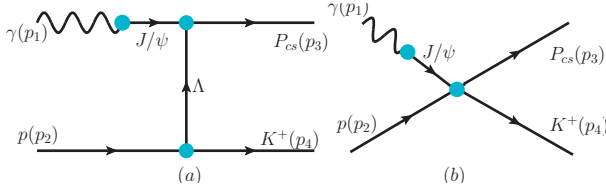


FIG. 2: Feynman diagrams for the process $\gamma p \rightarrow K^+ P_{cs}(4459)$ by assuming $P_{cs}(4459)$ as a compact pentaquark. The contributions from the t -channel Λ exchange (a) and contact term (b) are considered. We also show the definition of the kinematics (p_1, p_2, p_3, p_4) that we use in the present calculation.

effective Lagrangian with spin-parity quantum numbers for P_{cs} given [18]

$$\mathcal{L}_{P_{cs}\Lambda J/\psi}^{1/2^-} = -g_{P_{cs}\Lambda J/\psi} \bar{u}_{P_{cs}} \gamma_\mu \gamma_5 u_\Lambda J/\psi^\mu, \quad (28)$$

$$\mathcal{L}_{P_{cs}\Lambda J/\psi}^{3/2^-} = i \frac{g_{P_{cs}\Lambda J/\psi}}{2m_\Lambda} \bar{u}_{P_{cs},\mu} \gamma_\nu (\partial^\mu J/\psi^\nu - \partial^\nu J/\psi^\mu) u_\Lambda, \quad (29)$$

where the $g_{P_{cs}\Lambda J/\psi}$ is the coupling constant and can be determined by the decay width of $P_{cs} \rightarrow \Lambda J/\psi$

$$\Gamma(P_{cs}^{1/2^-} \rightarrow J/\psi\Lambda) = \frac{g_{P_{cs}\Lambda J/\psi}^2 |\vec{P}|_{J/\psi}}{8\pi m_{P_{cs}}^2 m_{J/\psi}^2} [m_{P_{cs}}^4 + m_{P_{cs}}^2 (m_{J/\psi}^2 - 2m_\Lambda^2) + 6m_{P_{cs}} m_{J/\psi}^2 m_\Lambda - 2m_{J/\psi}^4 + m_{J/\psi}^2 m_\Lambda^2 + m_\Lambda^4], \quad (30)$$

$$\Gamma(P_{cs}^{3/2^-} \rightarrow J/\psi\Lambda) = \frac{g_{P_{cs}\Lambda J/\psi}^2 |\vec{P}|_{J/\psi}}{288\pi m_{P_{cs}}^4 m_\Lambda^2} [3m_{P_{cs}}^6 - m_{P_{cs}}^4 (m_{J/\psi}^2 + 5m_\Lambda^2) + 12m_{P_{cs}}^3 m_{J/\psi}^2 m_\Lambda - m_{P_{cs}}^2 (m_{J/\psi}^4 - m_\Lambda^4) - (m_{J/\psi}^2 - m_\Lambda^2)^3]. \quad (31)$$

where $m_{J/\psi}$ is the mass of J/ψ meson. Using the corresponding strong decay width $\Gamma[P_{cs} \rightarrow \Lambda J/\psi] = 7.94$ MeV and the masses $m_{P_{cs}} = 4458$ MeV, we obtain $g_{P_{cs}\Lambda J/\psi}^{1/2^-} = 0.299$ and $g_{P_{cs}\Lambda J/\psi}^{3/2^-} = 0.453$.

The effective Lagrangians for the $J/\psi\gamma$ and ΛNK vertices are expressed as [18, 30]

$$\mathcal{L}_{\Lambda NK} = -\frac{f_{\Lambda NK}}{m_\pi} \bar{\Lambda} \gamma_\mu \gamma_5 N \partial^\mu K + H.c., \quad (32)$$

$$\mathcal{L}_{J/\psi\gamma} = \frac{em_{J/\psi}^2}{f_{J/\psi}} J/\psi_\mu \mathcal{A}^\mu, \quad (33)$$

where $m_\pi = 139.57$ MeV is the mass of the π^+ meson and $f_{\Lambda NK} = -0.2643$. There are several ways to determine the coupling constants $e/f_{J/\psi}$. In this work, we derive the coupling constant $e/f_{J/\psi} = 0.0221$ with the experimental partial decay width $\Gamma_{J/\psi \rightarrow e^+ e^-}$ [1].

With above details, the scattering amplitudes of the $\gamma p \rightarrow K^+ P_{cs}$ reaction can be written as

$$\mathcal{M}_a^{1/2^-} = i \frac{g_{P_{cs}\Lambda J/\psi} f_{\Lambda NK}}{m_\pi} \frac{e}{f_{J/\psi}} \bar{u}(p_3, s_3) \gamma_\mu \gamma_5 \frac{\not{q}_t + m_\Lambda}{q_t^2 - m_\Lambda^2} \not{p}_4 \gamma_5 \times u(p_2, s_2) (-g^{\mu\nu} + p_1^\mu p_1^\nu / m_{J/\psi}^2) \epsilon_\nu(p_1, s_1) \mathcal{F}_\Lambda(q_t), \quad (34)$$

$$\mathcal{M}_a^{3/2^-} = -i \frac{g_{P_{cs}\Lambda J/\psi} f_{\Lambda NK}}{2m_\Lambda m_\pi} \frac{e}{f_{J/\psi}} \bar{u}_\mu(p_3, s_3) (p_1^\mu \gamma^\nu - \not{p}_1 g^{\mu\nu}) \times \frac{\not{q}_t + m_\Lambda}{q_t^2 - m_\Lambda^2} \not{p}_4 \gamma_5 u(p_2, s_2) (-g^{\eta\rho} + p_1^\eta p_1^\rho / m_{J/\psi}^2) \times \epsilon_\rho(p_1, s_1) \mathcal{F}_\Lambda(q_t), \quad (35)$$

The contact term illustrated in Fig. 3(b) serves to keep the full amplitude gauge invariant. For the present calculation, we adopt the form

$$\mathcal{M}_b^{1/2^-} = -i \frac{g_{P_{cs}\Lambda J/\psi} f_{\Lambda NK}}{m_\pi} \frac{e}{f_{J/\psi}} \frac{2p_1 \cdot p_3 - m_{P_{cs}} + m_\Lambda}{q_t^2 - m_\Lambda^2} \times \bar{u}(p_3, s_3) \gamma^\mu \not{p}_4 u(p_2, s_2) \epsilon_\mu(p_1, s_1) \mathcal{F}_\Lambda(q_t), \quad (36)$$

$$\mathcal{M}_b^{3/2^-} = 0. \quad (37)$$

III. RESULTS

According to Refs [5–10], $P_{cs}(4459)$ may be a molecular state. However, currently, we cannot fully exclude other possible explanations such as a compact pentaquark state [11–14]. Further research is required to decide whether it is a molecular or compact multi-quark state. The photon coupling with a quark [23] is significantly different from the coupling of the photon to the molecular constituent $\bar{D}^* \Xi_c$ of $P_{cs}(4459)$ [24, 25]. Hence, a precise measurement of the photoproduction is useful to test different interpretations of $P_{cs}(4459)$.

We first consider the $P_{cs}(4459)$ as pentaquark molecule, its productions in the $\gamma p \rightarrow P_{cs}K^+$ reaction is evaluated. The mechanism including the t -channel K^- meson exchange, the u -channel Λ exchange, the contract term, and the s -channel

where the nucleon is considered as intermediate state. To make a reliable prediction for the cross-section of the process $\gamma p \rightarrow P_{cs}K^+$, two issues we need to clarify are, respectively, the relation of the parameters Λ_M , Λ_B , m and n to the form factors and the coupling of the $P_{cs}(4458)$ with $\gamma\Lambda$ and K^-p .

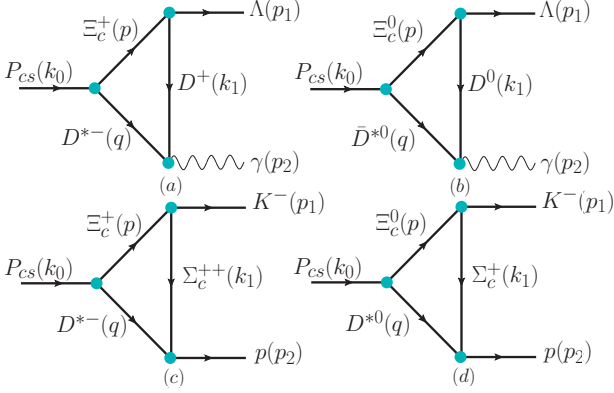


FIG. 3: Feynman diagrams for $P_{cs} \rightarrow \gamma\Lambda$ and K^-p decay processes. The contributions from the t -channel D exchange(a) and Σ_c exchange(b) are considered. We also show the definition of the kinematical $(k_0, p, q, p_1, p_2, k_1)$ that we use in the present calculation.

Unfortunately, there is no experimental information on the decay widths for $\Gamma(P_{cs} \rightarrow \gamma\Lambda)$ and $\Gamma(P_{cs} \rightarrow K^-p)$, as these are very difficult to determine. Thus, it is necessary to rely on theoretical predictions, such as those of Ref. [8]. The authors in Ref. [8] conclude that the total decay width of the $P_{cs}(4459)$ was reproduced with the assumption that $P_{cs}(4459)$ is a pure $\bar{D}^*\Xi_c$ bound state with $J^P = 1/2^-$, while in spin-parity $J^P = 3/2^-$ case may be S -wave coupled bound state with larger $\bar{D}^*\Xi_c$ component. Based on the molecular scenario, the partial decay widths of the $P_{cs}(4459)$ with $J^P = 1/2^-$ and $3/2^-$ into $\gamma\Lambda$ and K^-p final states through hadronic loops are evaluated with the help of the effective Lagrangians. The loop diagrams are shown in Fig. 3. The obtained partial decay widths are listed in Table I (more details can be found in the Appendix). With these decay widths, the coupling constants can be obtained, as in Table I.

TABLE I: The values of the partial decay widths and coupling constants for different J^P states.

Decay model	J^P	$\Gamma(\text{KeV})$	Coupling constants
$P_{cs}(4459) \rightarrow \gamma\Lambda$	$1/2^-$	63.83	$h = 0.035$
$P_{cs}(4459) \rightarrow \gamma\Lambda$	$3/2^-$	34.18	$h_1 = 0.05, h_2 = 0$
$P_{cs}(4459) \rightarrow K^-p$	$1/2^-$	2.05	$g_{KNP_{cs}} = 0.0041$
$P_{cs}(4459) \rightarrow K^-p$	$3/2^-$	0.24	$g_{KNP_{cs}} = 0.0017$

It is worth noting that the decay width of the process $P_{cs} \rightarrow \gamma\Lambda$ is larger than that of the process $P_{cs} \rightarrow K^-p$. A possible explanation for this may be that the decay of P_{cs} into $\gamma\Lambda$ should be easier via $c\bar{c}$ annihilation than via the Okubo-Zweig-Iizuka mechanism existing in the process $P_{cs} \rightarrow K^-p$. The larger $P_{cs} \rightarrow \gamma\Lambda$ decay in Fig. 3 also can be understood

due to the fact that the D -meson exchange plays the main role compared to the Σ_c -baryon exchange. This mainly originates from the idea that the meson exchange plays an indispensable role compared to the baryon exchanges in the hadrons interaction. Therefore, only π -meson exchange contribution is allowed in studying the nuclear force [26].

At present, the parameters Λ_M , Λ_B , m and n could not be determined by first principles. They are usually determined from the experimental branching ratios. The free parameters Λ_M , Λ_B , m and n are fixed by fitting the experimental data of the process $\gamma p \rightarrow K^{*+}\Lambda$ [27], by procedures illustrated in Ref. [22]. In this work, we adopt the values $\Lambda_M = [1.0, 1.019, 0.993, 1.030, 1.018]$ GeV, $\Lambda_B = 0.9$ GeV and $m = n = 2$ because these value are determined from the experimental data of Ref. [27] within the same K^- , p and Λ form factors adopted in the current work.

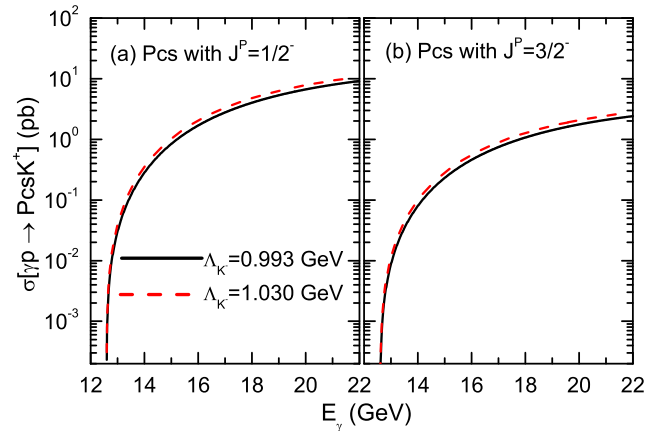


FIG. 4: (Color online) The total cross section for the process $\gamma p \rightarrow P_{cs}K^+$ with different Λ_{K^-} .

Once the model parameters and coupling constants are determined, the total cross section versus the beam momentum of the photon for $\gamma p \rightarrow P_{cs}K^+$ transition can be evaluated. In Fig. 4, the total cross section of process $\gamma p \rightarrow P_{cs}K^+$ with different Λ_{K^-} is presented, where we restrict the value of Λ_{K^-} by a reasonable range from 0.993 to 1.030 GeV. We find that the value of the cross section increases with the increasing of Λ_{K^-} . It is worth mentioning that the value of the cross section is not very sensitive to the model parameter Λ_{K^-} . To see how much it depends on the cutoff parameter Λ_{K^-} , as an example we take the cross section at an energy about $E_\gamma = 18.0$ GeV. The obtained cross section ranges from 4.02 pb to 4.77 pb for the process $\gamma p \rightarrow P_{cs}^{1/2^-} K^+$ and from 1.07 pb to 1.27 pb for the process $\gamma p \rightarrow P_{cs}^{3/2^-} K^+$. Hence, we only compute the total cross section of the process $\gamma p \rightarrow P_{cs}K^+$ with $\Lambda_{K^-} = 1.0$ GeV.

With $\Lambda_{K^-} = 1.0$ GeV, the total cross section for the beam momentum E_γ from reaction threshold up to 22.0 GeV are shown in Fig. 5. We find that the total cross section increases sharply near the K^+P_{cs} threshold. At higher energies, the cross section increases continuously but relatively slowly compared to the behavior near threshold. With the increase

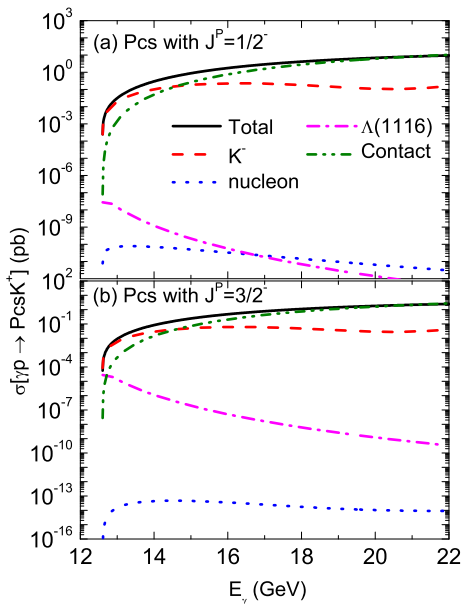


FIG. 5: (Color online) The cross section for the $\gamma p \rightarrow P_{cs}K^+$ reaction as a function of the beam momentum E_γ for (a) P_{cs} with $J^P = 1/2^-$ case and (b) the P_{cs} with $J^P = 3/2^-$ case. The contributions including the s -channel nucleon pole (blue dot line), the t -channel K^- exchange (red dash line), $\Lambda(1116)$ as an intermediate state in the u -channel (magenta dash dot line) and the contact term (olive dash dot dot line). The black solid line is the total cross section.

of the beam momentum, the total cross section increases. The results also show that the total cross section for P_{cs} production for $J^P = 1/2^-$ is larger than for $J^P = 3/2^-$. Taking the cross section at an energy about 19.00 GeV as example, the cross section is of the order of 5.515 pb for $P_{cs}^{J^P=1/2^-}$ production and 1.464 pb for $P_{cs}^{J^P=3/2^-}$ production. Such a result is very challenging to search for at EICC [16] but possible at US-EIC [17] due to a higher luminosity. We also find that the t -channel K^- meson exchange plays a predominant role near the threshold, while the contributions from the contact term become most important when the beam energy E_γ is larger than 14.63 GeV. Moreover, the line shapes of the cross-sections for those two case are the same.

Fig. 5 also tells us that the contributions from the s -channel nucleon pole and $\Lambda(1116)$ as an intermediate state in the u -channel are small. The interferences among them are quite small, especially at high energies, with the consequence that the t -channel K^- meson exchange and contact term contributions almost saturate the total cross section. From Eqs. 24 and 25, we can address that the dominant contribution from t -channel K^- exchange and negligible s -channel contribution make the contact term contribution become most important at high energies. The dominant K^- meson exchange contribution can be easily understood since the $P_{cs}^{1/2^-}$ and $P_{cs}^{3/2^-}$ are assumed as molecular state with a $\bar{D}^*\Xi_c$ component. Note that the molecule picture [5–10] is different from the compact pentaquark picture [11–13].

Our calculation indicates that the contributions from s -channel nucleon pole and u -channel $\Lambda(1116)$ exchange are quite small and the values are smaller than about the order of 10^{-5} pb. A possible explanation for this may be that the nucleon and $\Lambda(1116)$ are far off the threshold. It naturally reminds us of what could be the contribution of so many excited states of the nucleon and $\Lambda(1116)$, or other baryonic states in the light quark sector, which can enhance the cross section of $\gamma p \rightarrow P_{cs}K^+$ reaction make the EicC easily detect with current luminosity design. Unfortunately, there is no information on such studies. Thus, we do not consider the contributions from other states with heavier mass in this work.

Now we turn to the cross section for $\gamma p \rightarrow P_{cs}K^+$ by assuming $P_{cs}(4459)$ as a compact pentaquark. The cross section for the beam momentum E_γ from reaction threshold up to 22.0 GeV are shown in Fig. 6. We find that the total cross section increases sharply near the threshold. At higher energies, the cross section increases continuously but relatively slowly compared to the behavior near threshold. With the increase of the beam momentum, the total cross section increases. The results also show that the total cross section for P_{cs} production for $J^P = 1/2^-$ is much larger than for $J^P = 3/2^-$. Such as the total cross sections at an energy about $E_\gamma = 20.0$ GeV can reach 1509.36 pb for $P_{cs}^{J^P=1/2^-}$ production and 7.84 pb for $P_{cs}^{J^P=3/2^-}$ production. Moreover, the contributions from the contact term for $J^P = 1/2^-$ plays a predominant role, which almost equal to the total cross section.

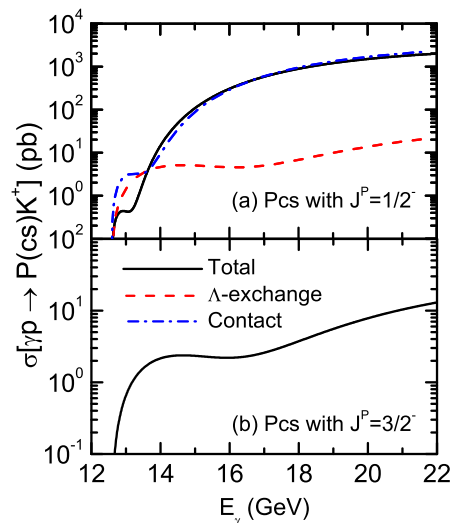


FIG. 6: (Color online) The cross section for the $\gamma p \rightarrow P_{cs}K^+$ reaction as a function of the beam momentum E_γ for (a) P_{cs} with $J^P = 1/2^-$ case and (b) the P_{cs} with $J^P = 3/2^-$ case by assuming $P_{cs}(4459)$ as a compact pentaquark. The contributions including the t -channel Λ exchange (red dash line) and the contact term (blue dash dot). The black solid line is the total cross section.

Comparing the cross-sections shown in Figs. 5 and 6, we can find that if the P_{cs} is produced as a compact pentaquark state, the cross-section and the line shapes of the cross-sections are different from the results that are obtained

by assuming $P_{cs}(4459)$ as $\bar{D}^*\Xi_c$ bound state. These differences will be very useful to help us to test various interpretations of the $P_{cs}(4459)$.

IV. SUMMARY

In this paper, we made a detailed exploration of the non-resonant contribution to the $\gamma p \rightarrow P_{cs}K^+$ reaction, intending to find a reasonable estimate of the P_{cs} production rates at relatively high energies, where no data are available up to now. The production process is described by the t -channel K^- exchange, s -channel nucleon pole, u -channel $\Lambda(1116)$ exchange, and the contact term. Based on the theoretical conclusion in Ref [8] that $P_{cs}(4459)$ can be interpreted as $\bar{D}^*\Xi_c$ bound state by studying the strong decay width, the coupling constants of the P_{cs} to γp and $K^- p$ needed in this work can be studied. The relevant Feynman diagrams are shown in Fig. 3 and the results are given in Table I. For comparison, the cross section for $\gamma p \rightarrow P_{cs}K^+$ is given also by assuming $P_{cs}(4459)$ as a compact pentaquark.

With assuming P_{cs} as a $\bar{D}^*\Xi_c$ bound state, the cross section for $\gamma p \rightarrow P_{cs}^{1/2^-}K^+$ and $\gamma p \rightarrow P_{cs}^{3/2^-}K^+$ reactions can reach 10.0 pb and 5.0 pb, respectively. However, the cross section for $\gamma p \rightarrow P_{cs}^{1/2^-}K^+$ and $\gamma p \rightarrow P_{cs}^{3/2^-}K^+$ reactions can reach 2000.0 pb and 13.0 pb, respectively, by considering P_{cs} as a compact pentaquark. Although the photoproduction cross-section is quite small, it is enough to test various interpretations of the $P_{cs}(4459)$ thanks to the low background of the exclusive and specific reaction proposed in this work. The future electron-ion colliders (EIC) of high luminosity in China ($2 - 4 \times 10^{33} \text{ cm}^{-2}\text{s}^{-1}$) [16] and the United States (US-EIC) ($10^{34} \text{ cm}^{-2}\text{s}^{-1}$) [17] provide a good platform for this purpose.

Acknowledgments

Yin Huang want to thanks for the support by the Development and Exchange Platform for the Theoretic Physics of Southwest Jiaotong University under Grants No.11947404 and No.12047576, the Fundamental Research Funds for the Central Universities (Grant No. 2682020CX70), and the National Natural Science Foundation of China under Grant No.12005177.

V. APPENDIX

In this appendix, we show how to compute the partial decay widths of $P_{cs} \rightarrow \gamma\Lambda$ and $P_{cs} \rightarrow K^-P$ reactions. The corresponding Feynman diagrams are shown in Fig. 3. To compute the diagrams, we require the effective Lagrangian densities for the relevant interaction vertices. The corresponding Lagrangian densities, theoretical formalism and coupling constants can be found in Ref. [8]. Here, we do not go into details.

The amplitudes for P_{cs} with $J^P = \frac{1}{2}^-$ case can be shown as

$$\begin{aligned} \mathcal{M}_a &= \bar{\mu}(p_1) \left(-\frac{e}{4\sqrt{2}} g_{\Xi_c^+ \Lambda D^+} g_{D^+ D^+ \gamma} g_{P_{cs}}^{1/2} \int \frac{d^4 k_1}{(2\pi)^4} \right. \\ &\quad \times \Phi((p\omega_{\bar{D}^{*-}} - q\omega_{\Xi_c^+})^2) \epsilon_{\mu\nu\alpha\beta} \gamma^5 \frac{\not{p} + m_{\Xi_c^+}}{p^2 - m_{\Xi_c^+}^2} \gamma^\sigma \gamma^5 \\ &\quad \times \frac{-g^{\lambda\sigma} + q^\lambda q^\sigma / m_{D^{*-}}^2}{q^2 - m_{D^{*-}}^2} (p_2^\mu g^{\theta\nu} - p_2^\nu g^{\theta\mu}) \\ &\quad \left. \times (q^\beta g^{\alpha\lambda} - q^\alpha g^{\beta\lambda}) \frac{1}{k_1^2 - m_{D^+}^2} \right) \epsilon^\lambda(p_2) \mu(k_0), \end{aligned} \quad (38)$$

$$\begin{aligned} \mathcal{M}_b &= \bar{\mu}(p_1) \left(\frac{e}{4\sqrt{2}} g_{\Xi_c^0 \Lambda D^0} g_{D^0 D^0 \gamma} g_{P_{cs}}^{1/2} \int \frac{d^4 k_1}{(2\pi)^4} \right. \\ &\quad \times \Phi((p\omega_{\bar{D}^{*0}} - q\omega_{\Xi_c^0})^2) \epsilon_{\mu\nu\alpha\beta} \gamma^5 \frac{\not{p} + m_{\Xi_c^0}}{p^2 - m_{\Xi_c^0}^2} \gamma^\sigma \gamma^5 \\ &\quad \times \frac{-g^{\lambda\sigma} + q^\lambda q^\sigma / m_{D^{*0}}^2}{q^2 - m_{D^{*0}}^2} (p_2^\mu g^{\theta\nu} - p_2^\nu g^{\theta\mu}) \\ &\quad \left. \times (q^\beta g^{\alpha\lambda} - q^\alpha g^{\beta\lambda}) \frac{1}{k_1^2 - m_{D^0}^2} \right) \epsilon^\lambda(p_2) \mu(k_0), \end{aligned} \quad (39)$$

$$\begin{aligned} \mathcal{M}_c &= \bar{\mu}(p_2) \left(\frac{1}{\sqrt{2}} g_{\Xi_c^+ \Sigma_c^{++} K^-} g_{D^+ p \Sigma_c^{++}} g_{P_{cs}}^{1/2} \int \frac{d^4 k_1}{(2\pi)^4} \right. \\ &\quad \times \Phi((p\omega_{\bar{D}^{*-}} - q\omega_{\Xi_c^+})^2) \gamma^\rho \frac{k_1 + m_{\Sigma_c^{++}}}{k_1^2 - m_{\Sigma_c^{++}}^2} \\ &\quad \times \gamma^5 \frac{\not{p} + m_{\Xi_c^+}}{p^2 - m_{\Xi_c^+}^2} \gamma^\sigma \gamma^5 \frac{-g^{\lambda\sigma} + q^\lambda q^\sigma / m_{D^{*-}}^2}{q^2 - m_{D^{*-}}^2} \left. \right) \mu(k_0), \end{aligned} \quad (40)$$

$$\begin{aligned} \mathcal{M}_d &= \bar{\mu}(p_2) \left(-\frac{1}{\sqrt{2}} g_{\Xi_c^0 \Sigma_c^+ K^-} g_{D^0 p \Sigma_c^+} g_{P_{cs}}^{1/2} \int \frac{d^4 k_1}{(2\pi)^4} \right. \\ &\quad \times \Phi((p\omega_{\bar{D}^{*0}} - q\omega_{\Xi_c^0})^2) \gamma^\rho \frac{k_1 + m_{\Sigma_c^+}}{k_1^2 - m_{\Sigma_c^+}^2} \\ &\quad \times \gamma^5 \frac{\not{p} + m_{\Xi_c^0}}{p^2 - m_{\Xi_c^0}^2} \gamma^\sigma \gamma^5 \frac{-g^{\lambda\sigma} + q^\lambda q^\sigma / m_{D^{*0}}^2}{q^2 - m_{D^{*0}}^2} \left. \right) \mu(k_0) \end{aligned} \quad (41)$$

and for $J^P = \frac{3}{2}^-$ have

$$\begin{aligned} \mathcal{M}_a &= \bar{\mu}(p_1) \left(i \frac{e}{4\sqrt{2}} g_{\Xi_c^+ \Lambda D^+} g_{D^+ D^+ \gamma} g_{P_{cs}}^{3/2} \int \frac{d^4 k_1}{(2\pi)^4} \right. \\ &\quad \times \Phi((p\omega_{\bar{D}^{*-}} - q\omega_{\Xi_c^+})^2) \epsilon_{\mu\nu\alpha\beta} \gamma^5 \frac{\not{p} + m_{\Xi_c^+}}{p^2 - m_{\Xi_c^+}^2} \\ &\quad \times \frac{-g^{\lambda\sigma} + q^\lambda q^\sigma / m_{D^{*-}}^2}{q^2 - m_{D^{*-}}^2} (p_2^\mu g^{\theta\nu} - p_2^\nu g^{\theta\mu}) \\ &\quad \left. \times (q^\beta g^{\alpha\lambda} - q^\alpha g^{\beta\lambda}) \frac{1}{k_1^2 - m_{D^+}^2} \right) \epsilon^\lambda(p_2) \mu^\sigma(k_0), \end{aligned} \quad (42)$$

$$\begin{aligned} \mathcal{M}_b &= \bar{\mu}(p_1) \left(-i \frac{e}{4\sqrt{2}} g_{\Xi_c^0 \Lambda D^0} g_{D^0 D^0 \gamma} g_{P_{cs}}^{1/2} \int \frac{d^4 k_1}{(2\pi)^4} \right. \\ &\quad \times \Phi((p\omega_{\bar{D}^{*0}} - q\omega_{\Xi_c^0})^2) \epsilon_{\mu\nu\alpha\beta} \gamma^5 \frac{\not{p} + m_{\Xi_c^0}}{p^2 - m_{\Xi_c^0}^2} \end{aligned}$$

$$\begin{aligned} & \times \frac{-g^{\lambda\sigma} + q^\lambda q^\sigma / m_{D^{*0}}^2}{q^2 - m_{D^{*0}}^2} (p_2^\mu g^{\theta\nu} - p_2^\nu g^{\theta\mu}) \\ & \times (q^\beta g^{\alpha\lambda} - q^\alpha g^{\beta\lambda}) \frac{1}{k_1^2 - m_{D^0}^2} \Big) \varepsilon^\lambda(p_2) \mu^\sigma(k_0), \end{aligned} \quad (43)$$

$$\begin{aligned} \mathcal{M}_c &= \bar{\mu}(p_2) \left(-i \frac{1}{\sqrt{2}} g_{\Xi_c^+ \Sigma_c^{*+} K^-} g_{D^{*-} p \Sigma_c^{*+}} g_{p_{cs}}^{1/2} \int \frac{d^4 k_1}{(2\pi)^4} \right. \\ & \times \Phi((p\omega_{D^{*-}} - q\omega_{\Xi_c^+})^2) \gamma^\rho \frac{k_1 + m_{\Sigma_c^{*+}}}{k_1^2 - m_{\Sigma_c^{*+}}^2} \\ & \left. \times \gamma^5 \frac{\not{p} + m_{\Xi_c^+}}{p^2 - m_{\Xi_c^+}^2} \frac{-g^{\lambda\sigma} + q^\lambda q^\sigma / m_{D^{*-}}^2}{q^2 - m_{D^{*-}}^2} \right) \mu^\sigma(k_0), \end{aligned} \quad (44)$$

$$\begin{aligned} \mathcal{M}_d &= \bar{\mu}(p_2) \left(i \frac{1}{\sqrt{2}} g_{\Xi_c^0 \Sigma_c^{*+} K^-} g_{D^0 p \Sigma_c^{*+}} g_{p_{cs}}^{1/2} \int \frac{d^4 k_1}{(2\pi)^4} \right. \\ & \times \Phi((p\omega_{D^0} - q\omega_{\Xi_c^0})^2) \gamma^\rho \frac{k_1 + m_{\Sigma_c^{*+}}}{k_1^2 - m_{\Sigma_c^{*+}}^2} \\ & \left. \times \gamma^5 \frac{\not{p} + m_{\Xi_c^0}}{p^2 - m_{\Xi_c^0}^2} \frac{-g^{\lambda\sigma} + q^\lambda q^\sigma / m_{D^0}^2}{q^2 - m_{D^0}^2} \right) \mu^\sigma(k_0), \end{aligned} \quad (45)$$

where $\omega_i = m_i/(m_i + m_j)$. In the above Lagrangians, the effective correlation function $\Phi(y^2)$ show the distribution of the components in the hadronic molecule $P_{cs}(4459)$ state. More-

over, the role of the correlation function $\Phi(y^2)$ also is to avoid the Feynman diagrams ultraviolet divergence, as the Fourier transform should vanish quickly in the ultraviolet region in the Euclidean space. We adopt the form as used in Refs. [28, 29],

$$\Phi(-p^2) \doteq \exp(-p_E^2/\alpha^2), \quad (46)$$

where p_E is the Euclidean Jacobi momentum. At present, the experimental total widths of the $P_{cs}(4459)$ that can be considered as a molecule can be well explained with $\alpha = 1.0$ GeV [8]. Therefore we take $\alpha = 1.0$ GeV in this work to compute the partial decay widths of $P_{cs} \rightarrow \gamma\Lambda$ and $P_{cs} \rightarrow K^-P$ reactions.

Once the amplitudes are determined, the corresponding partial decay widths can be obtained, which read

$$\Gamma(P_{cs} \rightarrow) = \int \frac{1}{2J+1} \frac{1}{32\pi^2} \frac{|\vec{p}_1|}{m_{P_{cs}}^2} |\bar{\mathcal{M}}|^2 d\Omega, \quad (47)$$

where the J is the total angular momentum of $P_{cs}(4459)$, $|\vec{p}_1|$ is the three-momenta of the decay products in the center of mass frame, the overline indicates the sum over the polarization vectors of the final hadrons. The Ω is the space angle of the final particle in the rest frame of $P_{cs}(4459)$.

-
- [1] P. A. Zyla *et al.* [Particle Data Group], PTEP **2020**, 083C01 (2020).
- [2] R. Aaij *et al.* [LHCb], Sci. Bull. **66**, 1278-1287 (2021).
- [3] R. Aaij *et al.* [LHCb], Phys. Rev. Lett. **115**, 072001 (2015).
- [4] R. Aaij *et al.* [LHCb], Phys. Rev. Lett. **122**, 222001 (2019).
- [5] H. X. Chen, W. Chen, X. Liu and X. H. Liu, Eur. Phys. J. C **81**, 409 (2021).
- [6] C. W. Xiao, J. J. Wu and B. S. Zou, Phys. Rev. D **103**, 054016 (2021).
- [7] F. Z. Peng, M. J. Yan, M. Sánchez Sánchez and M. P. Valderama, [arXiv:2011.01915 [hep-ph]].
- [8] F. Yang, Y. Huang and H. Q. Zhu, [arXiv:2107.13267 [hep-ph]].
- [9] J. T. Zhu, L. Q. Song and J. He, Phys. Rev. D **103**, 074007 (2021).
- [10] R. Chen, Phys. Rev. D **103**, 054007 (2021).
- [11] Z. G. Wang, Eur. Phys. J. C **76**, 142 (2016).
- [12] K. Azizi, Y. Sarac and H. Sundu, Phys. Rev. D **103**, 094033 (2021).
- [13] U. Özdem, Eur. Phys. J. C **81**, 277 (2021).
- [14] E. Santopinto and A. Giachino, Phys. Rev. D **96**, 014014 (2017).
- [15] F. Gursey and L. A. Radicati, Phys. Rev. Lett. **13**, 173-175 (1964).
- [16] D. P. Anderle, V. Bertone, X. Cao, L. Chang, N. Chang, G. Chen, X. Chen, Z. Chen, Z. Cui and L. Dai, *et al.* Front. Phys. (Beijing) **16**, 64701 (2021).
- [17] A. Accardi, J. L. Albacete, M. Anselmino, N. Armesto, E. C. Aschenauer, A. Bacchetta, D. Boer, W. K. Brooks, T. Burton and N. B. Chang, *et al.* Eur. Phys. J. A **52**, 268 (2016).
- [18] S. Clymton, H. J. Kim and H. C. Kim, Phys. Rev. D **104**, 014023 (2021).
- [19] Y. Huang, J. J. Xie, J. He, X. Chen and H. F. Zhang, Chin. Phys. C **40**, 124104 (2016).
- [20] Q. Wang, X. H. Liu and Q. Zhao, Phys. Rev. D **92**, 034022 (2015).
- [21] Y. Oh, C. M. Ko and K. Nakayama, Phys. Rev. C **77**, 045204 (2008).
- [22] A. C. Wang, W. L. Wang, F. Huang, H. Habersiz and K. Nakayama, Phys. Rev. C **96**, 035206 (2017).
- [23] R. Koniuk and N. Isgur, Phys. Rev. D **21**, 1868 (1980) [erratum: Phys. Rev. D **23**, 818 (1981)].
- [24] H. Zhu and Y. Huang, Chin. Phys. C **44**, 083101 (2020).
- [25] Y. Huang, F. Yang and H. Zhu, Chin. Phys. C **45**, 073112 (2021).
- [26] H. Yukawa, Proc. Phys. Math. Soc. Jap. **17**, 48 (1935), [Prog. Theor. Phys. Suppl. **1**, 1(1935)].
- [27] W. Tang *et al.* [CLAS], Phys. Rev. C **87**, 065204 (2013).
- [28] Y. Dong, A. Faessler, T. Gutsche and V. E. Lyubovitskij, Phys. Rev. D **77**, 094013 (2008).
- [29] Y. Dong, A. Faessler, T. Gutsche, Q. Lu and V. E. Lyubovitskij, Phys. Rev. D **96**, 074027 (2017).
- [30] Y. Huang, J. He, H. F. Zhang and X. R. Chen, J. Phys. G **41**, 115004 (2014).